Proceedings of ICMM2005
3rd International Conference on Microchannels and Minichannels
June 13-15, 2005, Toronto, Ontario, Canada

ICMM2005-75005

NUMERICAL SOLUTION OF TWO-FLUID ELECTROOSMOTIC FLOW

Yandong Gao, Y.F. Yap, T.N. Wong *, J.C.Chai, , C.Yang and K.T. Ooi
School of Mechanical and Production Engineering
Nanyang Technological University
Singapore 639798
*Correspondence author: Fax: (65) 6792-4062 Email: mtnwong@ntu.edu.sg

ABSTRACT

Two-fluid flows in microchannel are often found in biological analysis, such as during ion exchange or solvent extraction from one phase to another. In this article, a numerical scheme is presented to describe a two-fluid flow in microchannel with electroosmotic (EO) effects. In this two-fluid system, the interfacial viscous force of a high EO mobility fluid drags a low EO mobility fluid; the high EO mobility fluid is driven by electroosmosis. We particularly analyze the electric double layer (EDL) regions close to the wall and the interface in the high EO mobility fluid. As the governing equation of the electrical potential is singularly perturbed, finer meshes are adopted to capture these EDL regions.

In simulation, the interface between the two fluids evolves along the flow direction as the flow develops. Level set method is used to capture the interface implicitly. A localized mass preservation scheme is used to ensure mass conservation. A finite-volume method is used to solve the coupled electric potential equation, level set equations and Navier-Stokes equation.

The validity of the numerical scheme is evaluated by comparing its predictions with the results of the analytical solutions in the fully developed regions. The interface positions; pressure gradients; mass flow rates and velocity profiles of the two fluids along the channels are obtained numerically.

INTRODUCTION

Two-fluid electroosmotic flows are encountered in a variety of microfluidics. To induce electroosmosis, the working fluid is required to be a polar liquid with significant electrical conductivity, which is called high EO mobility fluid. Low EO mobility fluids such as oil cannot be pumped due to the low electrical conductivity. In some biochemical analysis, the electroosmosis may be unsuitable directly for the water solutions. This is because that the voltage applied to the solutions can lead to undesirable problems, i.e., the electrochemical decomposition of the solute, the fluctuation of the pH of the buffer solution and the generation of gases. Brask et al. [1] and Watanabe et al. [2], independently, proposed an idea to use the high EO mobility liquid as a driving mechanism to drag another liquid to avoid the above mentioned problems. A concept to control the interface location of a pressure driven two-liquid flow in a microchannel using electroosmotic flow effect was proposed by Wang et al [3]. Adjusting the magnitude and direction of the electric field had successfully controlled the interface position between the two liquids.

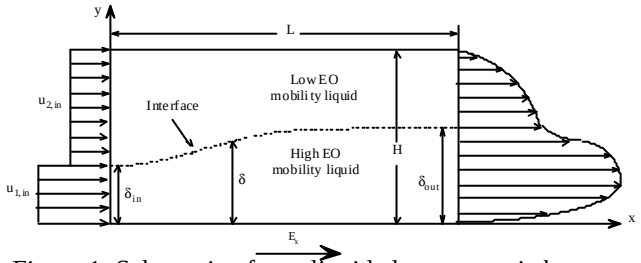

Figure 1: Schematic of two-liquid electroosmotic between parallel plates

In this work, we tested a numerical model for two-fluid electroosmotic flow. There are two immiscible fluids or two immiscible fluids with low diffusivity: a high EO mobility fluid at the bottom section and a low EO fluid at the upper section of the channel as shown in Fig.1. When an electric flied is applied across the channel, electroosmotic force will be generated in the high EO mobility fluid. Hence it affects the flow of two fluids. The flow of the two-fluid depends on the viscosity ratio, external electric field, electroosmotic characters of the high EO mobility fluid and interfacial curvature between them.

In this article, the level set (LS) method [4-6] is used to capture the interface. The local mass correction scheme of Yap et al. [7]

is used to ensure mass conservation of the two fluids at every cross section.

NOMENCLATURE

e	elementary charge
E	electric field intensity
$H_{\tilde{a}}$	Heaviside function
K	electric double layer parameter
k_b	Boltzmann constant
$\dot{m}_c$	current mass flowrate
$\dot{m}_{cor}$	mass preservation factor
$\dot{m}_d$	desired mass flowrate
n	multiplication factor
n_0	bulk concentration
N	total number of the mesh
t, t'	pseudo time
T	absolute temperature
u	velocity
V	electric voltage
x	coordinates
$\vec{x}$	position vector
z_0	valence of ions
$\acute{a}$	property
$\tilde{a}$	grid size related parameter
$\mathring{a}$	electric permittivity
$\hat{e}_D$	Debye length
$\grave{i}$	viscosity
$\tilde{n}$,	density
$\tilde{n}_e$,	net electric charge density
$\hat{i}$	level set function
æ_w,	zeta potential at the wall
$\grave{o}, \grave{o}'$	distance function
f	total electric potential
ö	externally applied electric potential
ø	electric potential due to surface charge

Subscripts

1	high EO mobility fluid
2	low EO mobility fluid
ref	reference quantity

Superscripts

–	dimensionless quantity

MATHEMATICAL FORMULATION

Governing Equations

Figure 1 shows the schematic of the problem considered in this article. The microchannel is filled with two (a high EO mobility and a low EO mobility) immiscible fluids. When an electric field is applied across the channel, the high EO mobility fluid will be driven by electroosmosis. The high EO mobility fluid then drags the second fluid along the microchannel affecting the flow of two-fluids.

For small Debye length and small zeta potential, the electric potential can be further decomposed into the potential due to the charge acquired at the wall ø, and the potential due to the externally applied electric field, ö [8]. The dimensionless continuity equation, momentum equations for steady incompressible Newtonian fluids and equations for potential due to applied electric field and potential due to surface charges in Cartesian tensor notation can be written as

$$\frac{\partial\left(r\,\bar{u}_j\right)}{\partial\bar{x}_j}=0 \qquad (1)$$

$$\mathrm{Re}\frac{\partial\left(\bar{u}_i\bar{u}_j\right)}{\partial\bar{x}_j}=-\mathrm{Re}\frac{\partial\bar{p}}{\partial\bar{x}_i}+\frac{\partial}{\partial\bar{x}_j}\left(\bar{m}\frac{\partial\bar{u}_i}{\partial\bar{x}_j}\right)+\frac{\partial}{\partial\bar{x}_j}\left(\bar{m}\frac{\partial\bar{u}_j}{\partial\bar{x}_i}\right)+K^2\sinh(\bar{y})\frac{\partial\bar{f}}{\partial\bar{x}_i} \qquad (2)$$

$$\frac{\partial^2\bar{y}}{\partial\bar{x}_j^2}=K^2\sinh\left(\bar{y}\right) \qquad (3)$$

$$\frac{\partial^2\bar{f}}{\partial\bar{x}_j^2}=0 \qquad (4)$$

In above equations, Re is the Reynolds number defined as $\mathrm{Re}=r_{\mathrm{ref}}V_{\mathrm{in}}\mathring{a}k_BT/z_0e\grave{i}_{\mathrm{ref}}^2$, K is the EDL parameter defined as $K=H/\hat{e}_D$, where $k_D=\left(\mathring{a}k_bT/2z_0^2e^2n_0\right)^{1/2}$ is the Debye length. Here we nodimensionalize the variables by scaling the length by the channel height H, the potential ö by the value of the potential applied at the inlet V_{in}, the potential ø by $(K_bT)/(z_0e)$, the velocity by $V_{\mathrm{in}}\mathring{a}K_bT/Hz_0e\grave{i}_{\mathrm{ref}}$ and the pressure by $\tilde{n}_{\mathrm{ref}}(V_{\mathrm{in}}\mathring{a}K_bT/Hz_0e\grave{i}_{\mathrm{ref}})^2$.

The boundary conditions for the velocities, electric potential due to externally applied electric field and electric potential due to charges on the wall are

Inlet ($x = 0$)

Velocities: $\bar{u}=\begin{cases}\bar{u}_{1,\mathrm{in}} & \bar{y}\le d_{in}\\ \bar{u}_{2,\mathrm{in}} & \bar{y}>d_{in}\end{cases},\ \bar{v}=0$

Electric Potentials: $\bar{f}=\bar{V}_{\mathrm{in}},\ \partial\bar{y}/\partial\bar{x}=0$

outlet ($x = L$)

Velocities: $\partial\bar{u}/\partial\bar{x}=0,\ \partial\bar{v}/\partial\bar{x}=0$

Electric Potentials: $\bar{f}=\bar{V}_{\mathrm{out}},\ \partial\bar{y}/\partial\bar{x}=0$

wall ($y = 0$)

Velocities: $\bar{u}=0,\bar{v}=0$

Electric Potentials: $\partial\bar{f}/\partial\bar{y}=0,\ \bar{y}=\bar{z}_w$

wall ($y = H$)

Velocities: $\bar{u}=0,\bar{v}=0$

Electric Potentials: $\partial\bar{f}/\partial\bar{y}=0$

interface($x = 0$)

Electric Potentials: $\bar{y}=0$

where V_{in} is the electric voltage at the inlet, V_{out} is the electric voltage at the outlet. $\bar{z}_w$ is the zeta potential at the wall contacting with the high EO mobility fluid. It is assumed that the wall in contact with the low EO mobility fluid does not acquire charges and interface does not touch the wall.

Therefore, we don't specify the boundary condition of y, at the wall(y=h). Instead, we specify the condition of y at the interface ($x = 0$). In the framework of the model, it is also assumed that there is no charge concentration at the fluid-fluid interface. The situation, where the interface holds certain electric charge, will be considered in the future work. We assumed two uniform velocities at the inlet for two liquids. The interface position of the interface, δ_{in}, is prescribed if Y-shape microchannel used.

Level Set Functions

The properties are calculated using

$$\bar{a} = (1 - H_g)\,\bar{a}_1 + H_g \bar{a}_2 \qquad (5)$$

In Eq. (5), $\bar{a}$ can be the density, viscosity or electric permittivity. The Heaviside function $H_{\tilde{a}}$ is related to the normal distance from the interface and is calculated using [5]

$$H_g = \begin{cases} 0 & x < -g \\ \dfrac{x+g}{2g} + \dfrac{1}{2p}\sin\left(\dfrac{px}{g}\right) & |x| \le g \\ 1 & x > g \end{cases} \qquad (6)$$

In Eq. (6), $\tilde{a}$ is related to the grid size and is usually taken as a factor of the grid spacing. The exact choice of $\tilde{a}$ will be explained later. $\hat{\imath}$ is the distance function which will be discussed in the following.

In this combined formulation, an additional scalar variable, called the level-set function, is used to identify the distances from the interface between the two fluids and the reference plane. The equation governing the evolution of the level-set function is

$$\bar{u}_j \frac{\partial x}{\partial \bar{x}_j} = 0 \qquad (7)$$

In the solution of the level-set function (Eq. 7), any convenient reference value can be assigned to the interface. The values of $\hat{\imath}$ at all node points are then calculated based on the reference value at the interface. The level-set function $\hat{\imath}$ is the *normal* distance from the interface. It is therefore a distance function which satisfies $|\nabla x| = 1$. The value of $\hat{\imath}$ at the interface is set to zero. As a result, $\hat{\imath}$ has opposite signs in the two fluids. For this formulation to work properly, $\hat{\imath}$ must remain a distance function. However, this can only be ensured at the beginning of the iteration process where the location of the interface is assumed and the values of $\hat{\imath}$ at all nodes are specified. During the iteration process, the values of $\hat{\imath}$ are calculated using Eq. (7). Although the interface is still represented by the reference value, the other values of $\hat{\imath}$ might not be the distances from the interface. As a result, another scalar variable is defined and solved. This variable must be a distance function and has the same interface value as $\hat{\imath}$. The "steady-state" solution of $\grave{o}$ given in Eq. (8) satisfies the above requirements.

$$\frac{\partial V}{\partial t} = \text{sign}(x)\left(1 - |\nabla V|\right) \qquad (8)$$

In Eq. (8), t is a *pseudo* time for the variable $\grave{o}$. Eq. (8) is subjected to the following initial condition.

$$V(\vec{x}, 0) = x(\vec{x}) \qquad (9)$$

It is clear from Eq. (8) that the "steady-state" solution satisfies $|\nabla V| = 1$. Thus, it is a distance function. The initial value (Eq. 9) ensures that the interface value of $\grave{o}$ is identical to the interface value of $\hat{\imath}$. As a result, the "steady-state" values of $\grave{o}$ are the distances from the interface. Although Eq. (8) ensures $\grave{o}$ and thus $\hat{\imath}$ as the distance function, it suffers a significant drawback. It does *not* ensure the conservation of mass of the various phases. To ensure mass conservation at *each* cross-section, a local mass correction factor is defined and an additional equation is solved [7]. This is written as

$$\frac{\partial V'}{\partial t'} = \dot{m}_{cor} \qquad (10)$$

In Eq. (10), t' and $\dot{m}_{cor}$ are pseudo-time (which can be different from the pseudo-time $\bar{t}$) and mass conservation factor, respectively. The local mass correction factor is

$$\dot{m}_{cor} = sign\left(x_{ref}\right)\frac{\left(\dot{m}_d - \dot{m}_c\right)}{\dot{m}_d} \qquad (11)$$

where $\dot{m}_d$ and $\dot{m}_c$ are the desired mass flowrate and the most current local mass flowrate of the reference phase, respectively. Depending on the choice of the Heaviside function of the reference phase, the mass flowrate of the reference phase can be calculated using

$$\dot{m} = \begin{cases} \sum r_{ref} H_g \, u \Delta A & H_{g,ref} = 1 \\ \sum r_{ref} \left(1 - H_g\right) u \Delta A & H_{g,ref} = 0 \end{cases} \qquad (12)$$

The summation is performed over a cross section. In the absence of phase change, the desired mass flowrate is calculated using the *inlet* condition.

Numerical Method

The continuity equation (Eq. 1), momentum equation (Eq. 2), electric potential equations (Eqs. 3 and 4), the level-set equations (Eqs. 7, 8 and 10) are special cases of a general transport equation

$$r\frac{\partial \Phi}{\partial t} + r u_j \frac{\partial \Phi}{\partial x_j} = \frac{\partial}{\partial x_j}\left(\Gamma \frac{\partial \Phi}{\partial x_j}\right) + S \qquad (13)$$

where $Ö$, $ñ$, $Ã$ and S are the dependent variables, density, diffusion coefficient and source term respectively. The finite-volume method of Patankar [9] is used to solve the transport equation given in Eq. (13). A staggered grid is used in this article. The scalar variables are stored at the centers of the control volumes, while the velocities are located at the control volume faces. In this article, the power-law of [9] is used to model the combined convection-diffusion effect in the momentum equations. The first-order upwind scheme is used to model the convection of the level-set equations. The SIMPLER algorithm is used to resolve the velocity-pressure coupling. The fully implicit scheme is used to discretize the transient term. The resulting algebraic equations are solved using the TriDiagonal Matrix Algorithm.

RESULTS AND DISCUSSIONS

The mathematical model presented in the previous section is validated by comparing with the exact solutions of Gao et al. [10]. Unless otherwise specified, the high EO mobility fluid is called fluid 1; while the low EO mobility fluid is called fluid 2. The high EO mobility fluid is also used to calculate reference

values for non-dimensionalization purposes. As seen in Fig. 1, the two fluids flow between two parallel plates of length L separated by a distance H. The height of fluid 1 is the entrance of the channel, $\ddot{a}_{\text{in}}$. When an external electric field is applied along the channel, the interface between two fluids evolves along the flow direction. The velocity profile and the interface position at every section change with the strength of the applied electric field, ions properties in the high EO mobility fluid and the zeta potential at the wall in contact with the high EO mobility liquid. Once fully developed, the velocity profile and the interface location become independent of the streamwise coordinate.

Validation of the numerical shceme

In modeling EO flow in microchannels, it is important that the EDL is captured accurately. The thickness of the EDL, $k_D = \left(e k_b T / 2 z_0^2 e^2 n_0\right)^{1/2}$, termed as Debye length, is in the order of 10nm-1ì m. The region of varying potential extends to a distance of about $3\hat{e}_D$ before the potential has decayed to about 2% of its value at the surface. On the other hand, the microchannels utilized in many lab-on-a-chip applications are between 1ì m and 100ì m. As a result, K ($K=H/\hat{e}_D$) is a big number and the electroosmotic forces are concentrated within a very thin region adjacent to a surface. Eq. (3) is a singularly perturbed equation. Finer meshes near these affected regions are needed to capture the EDL forces accurately. In this article, piecewise-uniform fitted mesh [11] in the transverse direction is applied to resolve the EDL. The mesh is defined as

$$\bar{y}_i = \begin{cases} 3i\Delta / N & i \le N/3 \\ \bar{y}_{i-1} + 3(1-\Delta)/2N & i > 2N/3 \end{cases} \qquad (14a)$$

with

$$\Delta = \min\left\{\frac{1}{3}, \frac{4}{K}\ln N\right\} \qquad (14b)$$

where N is the total number of the mesh. The piecewise-uniform mesh points in the region $4\hat{e}_D$ from the wall. In fact third of the mesh points are there, and so the EDL is resolved by this method. A typical mesh is shown in Fig. 2. In the following, $\tilde{a}$ in Eq. (6) is calculated as

$$g = n\frac{3(1-\Delta)}{2N} \qquad (15)$$

where n is an integrate number.

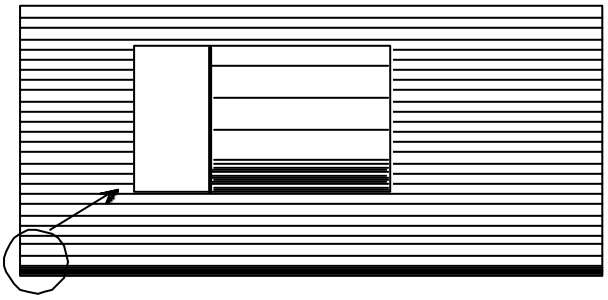

Figure 2: Schematic of the piecewise-uniform fitted mesh in y-direction

In the simulations, we fix the channel geometry H=100ì m and L=150ì m. The electric voltage at the inlet, V_{in}, is 0.75 volt and one at the outlet, V_{out}=0. The reference quantities $\grave{i}_{\text{ref}}$ and $\tilde{n}_{\text{ref}}$ are 10^{-3} Pa·s and 10^{3} kg·m^{-3}, respectively. At these conditions, the velocity scale is 9×10^{-5} m/s and the Reynolds number is about 3.6×10^{-3}.

For a set of given viscosity ratio (m_2/m_1), applied electric field, pressure gradient, the fully developed thickness of the high EO mobility fluid d_{out}/H, depends on the volumetric flowrate ratio (q_2/q_1) of the two fluids. For this verification, fluid 1 occupies 30% of the channel at the inlet and the volumetric flowrate ratio is fixed such that both fluids occupy half of the channel in the fully developed region.

The values of other parameters in this case are chosen as: K = 200, m_2/m_1 = 10, $\bar{z}_w = 0.2$. The inlet conditions are set such that the outlet is equally occupied by the two fluids.

Figure 3 shows the velocity field along the channel. The interface develops from 0.3 at inlet to 0.5 at outlet

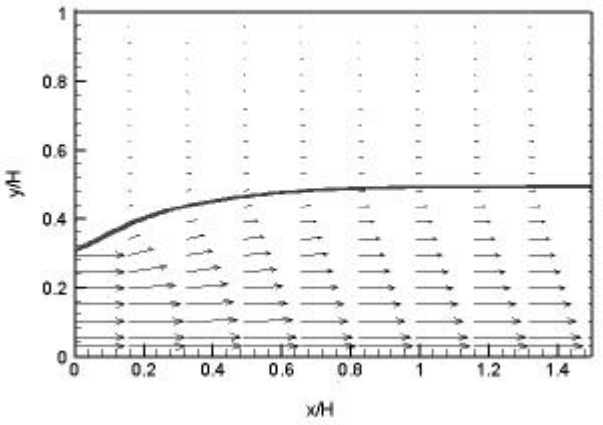

Figure 3: The velocity field along x/H

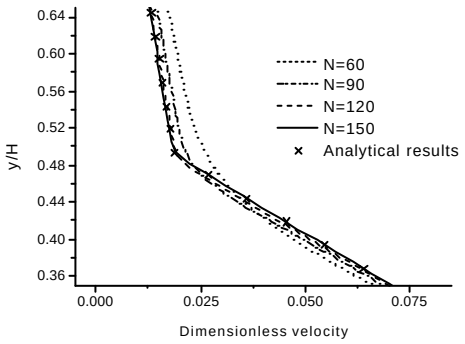

Figure 4: Velocity profiles for various meshes

Fig. 4 shows the detail comparisons of the fully developed velocity profile at outlet obtained using various computational grids with the exact solution when n=2. The results presented in Fig. 4 show the decay of discretization error with increased the total grid number N. It can be seen that the exact solution is reproduced accurately.

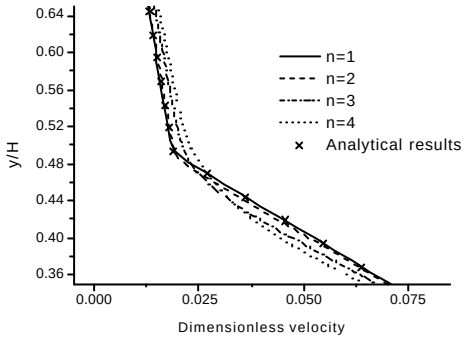

Figure 5: Velocity profiles for various values of *n*

Figure 5 shows the comparisons of the fully developed velocity profiles obtained using four values of *n* with the exact solution when the total grid number N=120. Under the same total number of grid N, a small value of *n* corresponds to a smaller transient region for the properties in Eq. (6), the velocity profile becomes sharper.

From all of above results, we can conclude that the interface evolution between two fluids is well captured and this numerical method is suitable. In the following simulations, N=120 and n=1 are used.

Electroosmotic Control of the Interface

For a set of given viscosity ratio (m_2/m_1), volumetric flowrate ratio and pressure gradient, the fully developed thickness of the high EO mobility fluid d_{out}/H, varies with the applied electric field. The values of parameters in this case are chosen as: K = 200, $\bar{z}_w = 4$, and same volumetric flowrate q_2/q_1=1. Figs. 6 and 7 show the evolutions of the interface and velocity profiles at the outlet for three different applied electric fields – no applied electric field, favorably and adversely applied electric field, respectively. The favorable electric field is applied as V_{in}=0.75volt and V_{out}=0, while the adverse one is applied as V_{in}=0 and V_{out}=0.75volt. Under favorably applied electric field, the electroosmotic forces will drag the high EO mobility liquid to facilitate its flow in the same direction of the pressure gradient. But adversely applied electric field will generate an opposite electroosmotic force and work against the pressure-driven flow.

For the pure pressure driven flow, the two liquids occupy half of the channel at the fully developed region (outlet) due to the same viscosity. As the electroosmotic force is concentrated in the EDL region close to the wall contacting with the high EO mobility liquid, the high EO liquid will flow faster in this region when a favorable electric field is applied. The average velocity of the high EO mobility liquid becomes faster. As the results, for the favorably applied electric field, the interface location at outlet becomes lower than the pure pressure driven flow. On the contrary, the high EO mobility liquid will bear an electroosmotic force against the flow direction. Apparently the high EO mobility fluid becomes more 'viscous' due to the adversely applied electric field. Therefore the high EO mobility liquid will occupy more portion of the channel than the pure pressure driven flow as shown in Figs. 6 and 7.

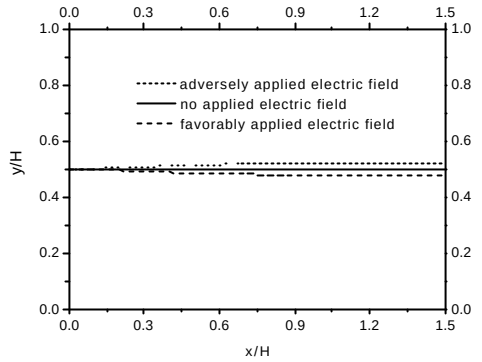

Figure 6: The interface profiles along x/H for m_2/m_1 = 1

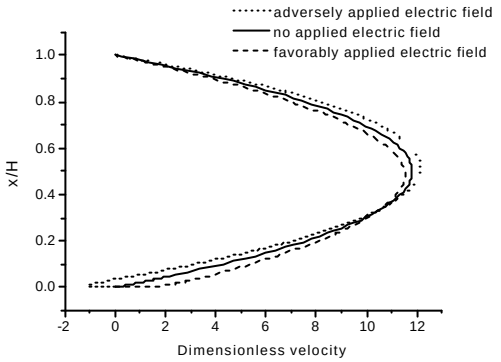

Figure 7: The velocity profiles at outlet for m_2/m_1 = 1

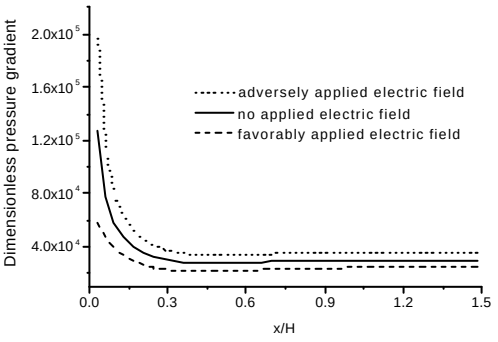

Figure 8: The pressure gradient along x/H for m_2/m_1 = 1

Two-fluid flow with an adversely electric field, the associated pressure gradient is highest as compare to favorably and no applied electric fields as depicted in Fig. 8. The result in Fig. 8 also highlighted that during the two-fluid development process excess pressure drop occurs due to the flow acceleration and the increased shear in the entrance boundary layers.

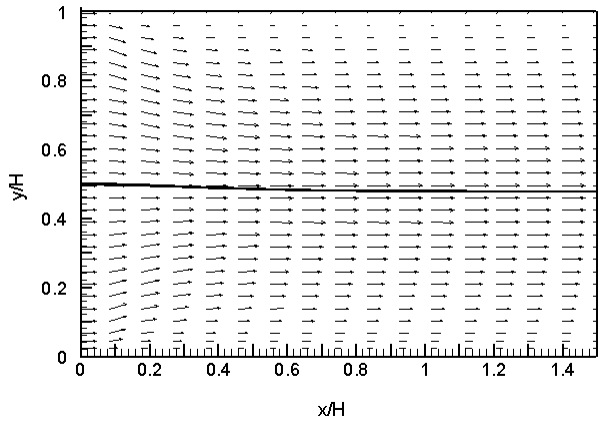

Figure 9: The velocity field along x/H under adversely applied electric field

Figure 9 shows the evolution of the two-fluid velocity field and interface field under the pressure driven with adversely applied electric field. It can be seen that the present procedure captures the interface location and resolve the EDL correctly.

CONCLUDING REMARKS

We presented numerical simulations results for two-liquid electroosmotic flow in a straight channel. The simulations are performed for specified inlet flowrate conditions and the electroosmotic forces are applied locally. The simulation results demonstrate the interface locations of a pressure-driven two-liquid flow in a microchannel can be controlled by using the electroosmotic flow effects. This concept has potential application for switching and cell sorting in bioanalytical systems.

ACKNOWLEDGMENTS

Yandong Gao gratefully acknowledges the PhD scholarship from Nanyang Technological University.

REFERENCES

[1] A. Brask, G. Goranovic, and H. Bruus, "Electro-osmotic pumping of nonconduction liquids by viscous drag from a secondary conducting liquid", In NanaTech 2003, proc., vol. 1, pages 190–193, San Francisco, USA, February 2003

[2] M. Watanabe, H. Shirai, and T. Hirai, "Liquid-liquid two-layer electrohydrodynamic flow system", *Sensors and Actuators B*, 94:267–270, 2003

[3] C. Wang, N.-T. Nguyen, and el al., 'Interface location control of pressure-driven two-fluid in a microchannel using electroosmosis effect', submitted

[4] S. Osher and J. A. Sethian, "Fronts propagating with curvature-dependent speed: Algorithms based on Hamilton-Jacobi formulations", *Journal of Computational Physics*, 79:12–49, 1988

[5] M. Sussman, P. Smereka, and S. Osher, "A level set approach for computing solutions to incompressible two-phase flow", *Journal of Computational Physics*, 114(1):146–159, 1994

[6] Y. C. Chang, T. Y. Hou, B. Merriman, and S. Osher, "A level set formulation of eulerian interface capturing methods for incompressible fluid flows", *Journal of Computational Physics*, 124(2):449–464, 1996

[7] Y.F. Yap, J. C. Chai, et. al., 'Numerical modeling of unidirectional stratified flow with and without phase change', in press, *Int. Journal of Heat and Mass Transfer*, 2004

[8] N. A. Patankar, and H. H. Hu, 'Numerical simulation of electroosmotic flow', *Analytical Chemistry*, 70:1870-1881, 1998

[9] S. V. Patankar, "*Numerical Heat Transfer and Fluid Flow*", Hemisphere Pub. Corp, Washington, 1980. ISBN 0-07-048740-5.

[10] Y. Gao, T. N. Wong, C. Yang, and K. T. Ooi, "Two-fluid electroosmotic flow in microchannel", in press, *Journal of Colloid and Interface Science*, 2004.

[11] P. Farrell, A. Hegarty, J. Miller, et al., "*Robust Computational Techniques for Boundary Layers*", Chapman & Hall/CRC, Boca Raton, 2000. ISBN 1-58-488192-5